ELSEVIER

Chemical Physics 205 (1996) 167–178

Chemical Physics

Ultrafast dynamics and structure at aqueous interfaces by second harmonic generation

X. Shi [1], E. Borguet, A.N. Tarnovsky, K.B. Eisenthal *

Department of Chemistry, Columbia University, New York, NY 10027, USA

Received 27 July 1995

Abstract

Femtosecond time-resolved second harmonic generation studies of the barrierless isomerization of an organic dye, malachite green (MG), have been carried out at several aqueous interfaces. A comparison of the dynamics at the air/aqueous, alkane/aqueous and silica/aqueous interfaces, indicates increased friction and increased water structure at the aqueous interfaces relative to bulk water, in support of molecular simulations, with the silica/aqueous interface being the most structured. The dynamics are slower at all of these interfaces than in bulk water, by a factor of three to five in the case of the air/aqueous and alkane/aqueous interfaces, and almost an order of magnitude in the case of the silica/aqueous interface. These investigations also indicate that the generally accepted isomerization model of twisting of the three aromatic rings about the central carbon atom requires modification in that the synchronous twisting of all three aromatic rings is not necessary for rapid internal conversion from the excited to ground electronic state. In contrast to MG, the dynamics of the activated photoisomerization of the cyanine dye, 3,3′-diethyloxadicarbocyanine iodide (DODCI), is faster at the air/aqueous interface than in bulk aqueous solution. The different dynamics of MG and DODCI suggest that the interface friction must be described in terms of the orientation and solvent structure in the vicinity of the chromophores involved in the isomerization process.

1. Introduction

The interface is that special region that provides the bridge between different bulk media. It is a subject of intense activity because of its scientific, environmental and technological importance [1–8]. The asymmetry of the forces at the interface, exemplified by the observation that molecules at liquid surfaces are aligned in a preferential direction rather than randomly oriented as they are in the bulk, is the origin of the unique chemical and physical properties of this region [9,10]. It has been demonstrated experimentally that fundamental chemical behavior, e.g., acidity (pH) [11] and equilibrium constants [12], are dramatically different at the interface. New physical behavior such as structural phase transitions involving the geometrical rearrangement of small mutually soluble molecules at liquid interfaces has been observed [13]. It is not surprising that the dynamics of chemical and physical processes, which depend on the properties of the medium in which they occur, should also differ at interfaces [14–16].

---

* Corresponding author.

[1] Present address: Department of Chemistry, University of Michigan, Ann Arbor, MI 48109, USA.

SSDI 0301-0104(95)00373-8

A major obstacle to the application of spectroscopic techniques to interface investigations is the necessity to differentiate between the response of the overwhelming number of bulk molecules and that of the much smaller number of surface molecules. Traditional spectroscopic methods such as emission spectroscopy can be used to study interface phenomena provided that the molecules of interest are restricted to the interface region [17,18]. There have been some successes in reducing bulk contributions by using a total internal reflection (TIR) geometry [19,20]. However, molecules present to a depth of over 100 nm contribute to the observed signals rendering a limited sensitivity to the separation of surface versus bulk effects.

Second harmonic generation, (SHG), is a method that avoids the complications of bulk contributions and permits surface species to be probed directly [1,6,8]. Using time resolved second harmonic generation, which is a pump–probe method, progress has been made in our understanding of elementary molecular processes at interfaces [1,6]. A study of the rotational motion of rhodamine 6G, an organic molecule, at the air/aqueous interface showed that the dynamics is slower than in the bulk, is dominated by out of plane molecular motions and that the ground and excited molecules have different orientations at the interface [16]. Time-resolved SHG (TRSHG) has also been used to investigate the dynamics of barrier crossing processes. In the case of the photoisomerization of the cyanine dye DODCI (3,3′-diethyloxadicarbocyanine iodide) at the air/aqueous interface the rate was measured and found to be considerably faster than in the bulk [14]. TRSHG has been employed to probe the photophysics of a number of molecules, including rhodamine 6G and malachite green, at silica/liquid and silica/air interfaces [19,21]. In the case of rhodamine 6G at the silica/aqueous interface, two relaxation components were observed; an 80 ps recovery attributed to surface dimers due to high surface coverage and a longer (~ 4 ns) component typical of bulk fluorescence dynamics. Studies of intermolecular electronic energy transfer at an air/liquid interface have been performed at bulk concentrations such that the energy transfer is among the interface molecules and energy transfer between the interface and bulk molecules can be neglected. The experimental results are consistent with our understanding of energy transfer process in the bulk [15]. Again, the use of SHG enabled the surface response to be probed exclusively. Ultrafast vibrational dynamics at interfaces have also been investigated using the related nonlinear optical technique, time-resolved IR–visible sum frequency generation (SFG) [22,23].

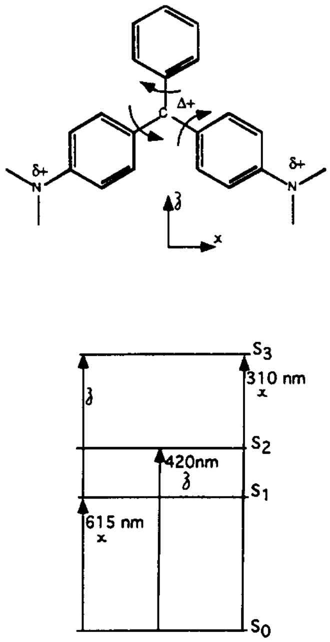

Scheme 1. Malachite green and its electronic states.

To complement our study of the photoisomerization of the cyanine dye, DODCI, where both a barrier and frictional effects determine the dynamics of the reaction, we initiated a study of the photoisomerization of malachite green (see Scheme 1), a barrierless process, at various aqueous interfaces. Our investigations seek to increase our knowledge of the effects of frictional resistance on molecular motions and the dynamics of chemical reactions at interfaces. As the MG reaction does not involve a barrier, it is the frictional effects at the interfaces that control the dynamics of the reaction. Such barrierless transformations constitute an important class of chemical isomerization dynamics, of relevance to primary electron transfer in the photosynthetic reaction center, oxygen transport by hemoglobin and fundamental mechanisms of vision [24]. For these processes the kinetics are determined not by the presence of barriers that separate different configurational regions but chiefly by interactions with the surrounding molecules (frictional effects) and the shape and intersections of the potential energy surfaces of different electronic states. The photoisomerization of malachite green, a triphenylmethane dye, has been extensively studied both in bulk media [25] and adsorbed on solid surfaces [19,21,26–30]. The ultrafast relaxation dynamics of triphenylmethane dyes in the bulk have been shown to be very sensitive to the nature of the molecular environment [25]. The fluorescence quantum yield and excited state relaxation rate show a strong dependence on solvent viscosity, whereas the effect of solvent polarity is not found to be significant based on similar dynamics in solvents of similar viscosities but very different polarity [31,32]. The weak solvent polarity dependence suggests that the potential energy surfaces are likely to be similar in the bulk and at the various interfaces studied. Pressure dependent bulk studies of triphenylmethane dyes also indicate that viscosity controls the barrierless torsional dynamics [33–35]. The ultrafast dynamics ($\sim 10^{-12}$ s) and apparent lack of a temperature dependence, under conditions of constant viscosity, in low viscosity solvents indicate that the relaxation is barrierless. The rate limiting step is believed to involve the rotation of the aromatic groups about the bond between each aromatic group and the central carbon atom (see Schemes 1 and 2) [36,37]. The solvent drag forces opposing these rotations are manifested by the slowing down of the isomerization as the macroscopic bulk solvent viscosity increases. A number of theories have been developed to account for the experimental observations. Most assume that the dynamics involve diffusional motion on an excited state potential surface until a sink is encountered, at which point internal conversion to the ground state occurs [38–41]. While the overwhelming consensus is that, in low viscosity solvents, the ground state recovery dynamics are mono-exponential and the rate decreases with viscosity, an absence of viscosity dependence was observed in one study [42]. Several reports of bi-exponential behavior [43,44] have been ascribed to saturation effects [45]. In spite of much experimental and theoretical work, important aspects of the isomerization, especially the relative contributions of the three aromatic groups remain to be determined [24]. It is clear, nevertheless, that when the aromatic rings are not free to rotate, as in the structurally related dyes such as rhodamine B, where the anilino rings are connected by an oxygen atom, there is no rapid excited state relaxation.

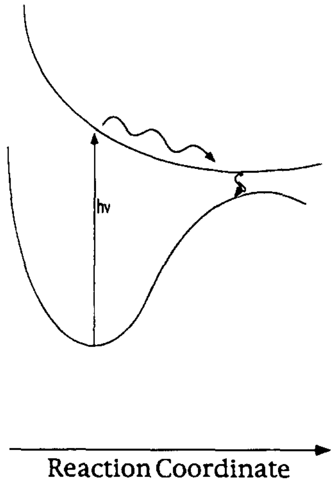

Scheme 2. Schematic of malachite green ground and excited electronic state dynamics. Upon absorption of a visible photon, malachite green undergoes motion along the reaction coordinate, involving torsion of the aromatic rings, effecting internal conversion to ground state.

Studies of the relaxation of malachite green molecules at the silica/air interface by second harmonic methods, revealed a fast decay component and a coverage dependent slow component of uncertain origin [19,21,29,30]. The fast component, though slower than the bulk relaxation times found in low viscosity liquids, was attributed to the intramolecular twisting motions of the aromatic rings about the central carbon atom. The details of the adsorbate geometry at the interface and the effects of intermolecular adsorbate–adsorbate interactions on the relaxation dynamics are important and need to be further investigated. Other studies of the fluorescence of malachite green molecules in the vicinity of the silica/aqueous interface ($\sim$ 100 nm) carried out in a total internal reflection geometry showed that there were slow, concentration dependent, components in the observed kinetics [26].

In the experiments described in this work the surface densities were sufficiently low, ~ 1000 Å^2/molecule, to avoid adsorbate–adsorbate interactions. Furthermore, the use of a femtosecond laser

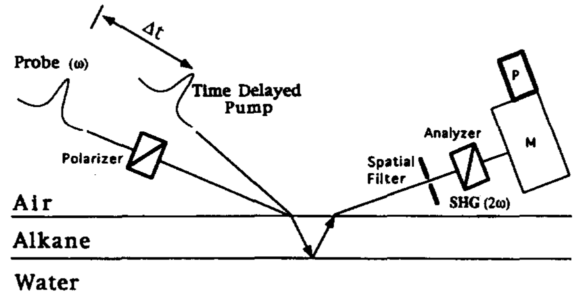

Fig. 1. Schematic of experimental setup.

system made it possible to observe the fast relaxation decay without the need for deconvolution methods. Our findings are that the barrierless isomerization dynamics of malachite green is significantly faster in bulk water than at the various interfaces studied, indicating that the friction is greater at the interfaces. The relaxation is almost an order of magnitude slower at the silica/water interface (5.5 ps) than in bulk water (0.7 ps), a factor of three slower at the air/water interface (2.0 ps) and a factor of four to five slower at the alkane/water interfaces (3.0–3.6 ps). Because the dynamics is friction controlled we were surprised to find that the kinetics changed by only ~ 20% in going from an octane/H_2O interface (3.0 ps) to a pentadecane/water interface (3.6 ps). The viscosities of octane and pentadecane differ by a factor of six and were expected to markedly change the twisting relaxation dynamics about the central carbon–phenyl bond because the phenyl group projects into the alkane phase. This latter result at the alkane/water interface brings into question the presently accepted model of isomerization which assumes that the synchronous rotations of all three aromatic rings are necessary. It is the selective and anisotropic interactions of an interface with different parts of a molecule that make it possible to investigate how the different chromophores contribute to the relaxation process. In this study it is the hydrophobic phenyl group projecting into the alkane phase and the anilino groups having net positive charge projecting into the water phase that permit separating the frictional effects exerted on different parts of the molecule.

2. Experimental

A 10 Hz amplified colliding-pulse mode-locked dye laser provides 130 fs pulses at 625 nm [46]. The

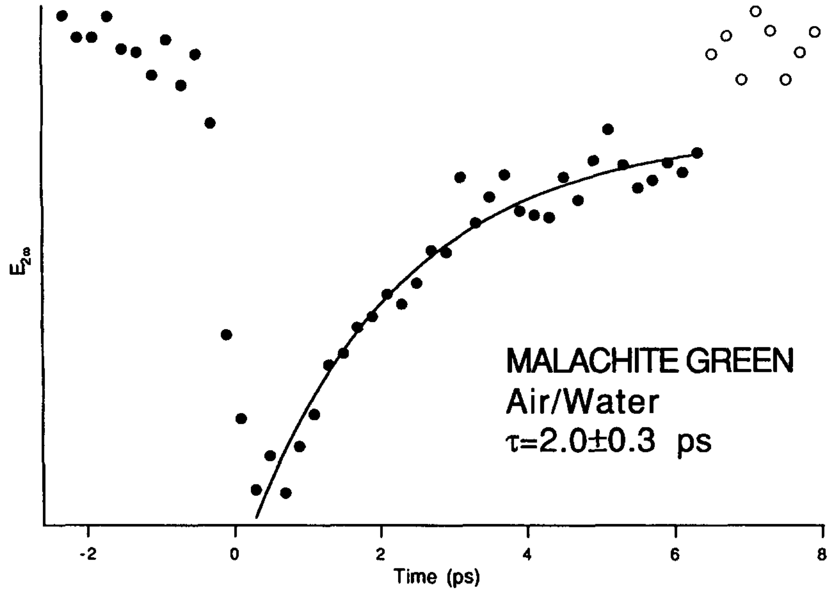

Fig. 2. TRSHG dynamics of malachite green at air/water interface. The solid line is a single exponential fit to the data. The last ten points ($t > 7$ ps, open circles) are obtained with the pump blocked, thus showing a small offset discussed in the text.

pump/probe approach employed is illustrated in Fig. 1. Probe energy densities of 0.1 to 1 mJ/cm^2 were used. The pump energy was typically three times or greater than the probe. The laser probe light is focused at the interface and the second harmonic radiation (312.5 nm) is separated from the reflected fundamental using filters and a monochromator (M), and detected using a gated photomultiplier (P). The pump and probe beams, both incident at 70° to the surface normal, propagate in slightly different directions to enable spatial separation of the SH radiation generated by each beam. The liquid–air and liquid–liquid interface experiments were performed on samples contained in teflon beakers. Experiments at the fused silica/aqueous interface used a teflon sample cell tightly covered with a fused silica equilateral prism (Esco). This prism was prepared as described previously [47]. The angle of incidence is different at the silica/water (66.9°), octane/water (42.3°) and pentadecane/water (41.0°) interfaces due to refraction. It should be noted that the geometry employed ensures total internal reflection in the case of the silica/water interface for which the critical angle (θ_c) is 65.9°, but not for the octane/water ($\theta_c = 72°$) or pentadecane/water ($\theta_c = 68.2°$) interfaces. Polarizers enable distinct components of the surface nonlinear susceptibility to be probed. Aqueous solutions of malachite green chloride (Aldrich, used as received) in doubly distilled water were prepared. The bulk acidity was controlled using hydrochloric acid (Amend Drug And Chemical Co.) solutions. Solution pH was 2.4 unless otherwise indicated. Gibbs surface excess at the air/aqueous interface was determined from surface tension measurements using the Wilhelmy plate method [48]. Alkanes (Aldrich, 99 + % purity) were used as received.

3. Results and discussion

The TRSHG dynamics observed at the air/aqueous interface, following promotion of malachite green to its first excited electronic state (S_1), are shown in Fig. 2. We estimate, from surface tension measurements that the surface coverage is approximately 10^{13} molecules/cm^2 for the 100 μM solution used in the experiments reported in Fig. 2. The TRSHG dynamics were independent of concentration in the range investigated (100–200 μM) and independent of energy density in the range studied.

Malachite green in the bulk has pH dependent equilibria among the monocation MG^+, the species generally referred to as malachite green, the dication MG^{2+} and the colorless carbinol form MGOH [25]. At low pH (< 1.5) it exists as a doubly charged cation (MG^{2+}) which absorbs in the blue and is therefore not resonant with the CPM laser used. At higher pH (> 7) malachite green exists predominantly as the carbinol (MGOH). The conversion process to MGOH is slow, but reversible, and is the origin of the alkaline fading of triphenylmethane dyes. Indeed, at pH > 4, the surface tension of aqueous malachite green solutions decreased with time, at constant bulk concentration, due to the formation of MGOH, sparingly solubility in water, and its adsorption to the interface. To ensure that we are investigating the properties of MG^+ the experiments were carried out at a bulk pH = 2.4.

We found that molecular rotation at the interface is not significant on the timescale of the isomerization kinetics at the interface from the observation that the polarization of the second harmonic light did not change with delay between the pump and probe light pulses. This observation is consistent with previous TRSHG measurements which revealed that diffusional molecular motion at the air/aqueous interface for molecules of comparable size and charge is only significant on timescales greater than one hundred picoseconds [16]. The isomerization dynamics were best characterized by a single exponential decay (2.0 ± 0.3 ps at the air/aqueous interface). These rates are significantly slower than the dominant decay component of ~ 0.7 ps reported for malachite green in bulk water [49–51].

The generally accepted model for the photoisomerization of TMP dyes in bulk solution involves the intramolecular rotations (twisting) of the aromatic groups about their respective bonds with the central carbon atom (Schemes 1 and 2) [24,25]. This motion is initiated by the change in the charge distribution of the molecule following excitation to the first excited singlet state. Although the frictional resistance exerted by the solvent against the twisting of the aromatic moieties in the bulk isomerization dynamics is seen in the viscosity dependence of the kinetics, the contribution of the individual groups is not known [36]. As noted earlier the solvent polarity is not observed to play a significant role in TMP relaxation dynamics as similar dynamics were observed in solvents of comparable viscosity yet greatly different dielectric constants and values of the solvent polarity parameter ET(30) [31,32]. We expect that the isomerization at the interface will also be sensitive to the friction experienced along the twisting coordinates.

3.1. Molecular orientational structure of malachite green at liquid interfaces

The intramolecular twisting motions of the aromatic groups that drive the relaxation process occur in the orientationally asymmetric environment of the interface. Because of this asymmetry the frictional resistance and thereby the isomerization kinetics can be dependent on the orientation of the molecule at the interface. It is therefore necessary to determine the molecular orientation of malachite green at the various interfaces to be investigated.

To obtain the molecular orientation the measured second order susceptibility elements, which are defined by the laboratory axes (X,Y,Z), must be related to the molecular axis system of the molecule at the interface [52,53]. This relation is contained in the expression

$$\chi^{(2)} = N_s \langle \alpha^{(2)} \rangle, \tag{1}$$

where N_s is the surface density of malachite green molecules, $\alpha^{(2)}$ the molecular polarizability and the brackets indicate an average over the orientational distribution of molecules at the interface. The laboratory axis system is defined by the interface normal (Z) and the plane of incidence (ZX). The in-plane isotropy of a liquid interface restricts the number of independent $\chi^{(2)}$ elements to three; χ_{ZZZ}, χ_{ZXX} and χ_{XZX}, where X and Y are equivalent. The three aromatic groups twisted in propeller like fashion about the central carbon–phenyl bonds yields a C_2 symmetry for malachite green with the following nonzero elements; $\alpha^{(2)}_{zzz}$, $\alpha^{(2)}_{zxx}$, and $\alpha^{(2)}_{xzx}$. z is the molecular symmetry axis and x is the axis in the plane defined by the bonds of the three aromatic groups to the central carbon atom. The relative importance of the different elements of the molecular polarizability can be predicted, in a first approximation, by examination of the electronic states of malachite green, schematically illustrated in Scheme 1. The $\alpha^{(2)}$ components containing the y axis are very small compared to those with the z and x axis elements, because the y axis transitions are in the far ultraviolet. Resonances exist along the x and z molecular axes at the laser fundamental wavelength ($\lambda = 625$ nm), for $S_0 \rightarrow S_1$ and $S_1 \rightarrow S_3$ respectively, and along the x molecular axis near the second harmonic wavelength ($\lambda = 312.5$ nm) for $S_0 \rightarrow S_3$. The values of the molar extinction coefficients were determined from UV–VIS measurements to be $\epsilon \sim 8 \times 10^4$ ℓ mol^{-1} cm^{-1} and $\epsilon \sim 2 \times 10^4$ ℓ mol^{-1} cm^{-1} for the $S_0 \rightarrow S_1$ and $S_0 \rightarrow S_3$ transitions, respectively. The excited state $S_1 \rightarrow S_3$ transition is significantly weaker than $S_0 \rightarrow S_1$ at the laser wavelength, 625 nm, as indicated by transient bleaching results from previous studies [50,51] and the efficacy of malachite green as a saturable absorber. Because of a resonant enhancement at both the fundamental and second harmonic wavelengths, the dominant components of the molecular polarizability are then $\alpha^{(2)}_{xzx}$ and $\alpha^{(2)}_{xxz}$, which are equal by symmetry. A smaller contribution is expected from $\alpha^{(2)}_{zxx}$ which is only resonant at the fundamental wavelength. The enhancement in the SH signal due to a double resonance relative to that of single resonance is found to be 100 from experiments on a related dye molecule [54].

The components of the macroscopic second order susceptibility $\chi^{(2)}$ expressed in terms of projections of the dominant molecular polarizability component $\alpha^{(2)}_{xzx}$ on the laboratory axes, described by means of the Euler angles (θ,ϕ,ψ) [55], yields

$$\chi_{ZZZ} = 2N_s \alpha^{(2)}_{xzx} \langle \cos\theta \sin^2\theta \rangle, \tag{2}$$

$$\chi_{ZYY} = \chi_{ZXX} = -N_s \alpha^{(2)}_{xzx} \langle \cos\theta \sin^2\theta \rangle, \tag{3}$$

$$\chi_{XZX} = \chi_{YZY} = \chi_{XXZ} = \chi_{YYZ} = -\frac{N_s}{2} \alpha^{(2)}_{xzx} (2\langle \cos\theta \sin^2\theta \rangle - \langle \cos\theta \rangle). \tag{4}$$

The angle between the surface normal (Z) and the molecular axis (z) is given by θ. We select $\psi = 90°$, the azimuthal angle about the molecular z axis, based on previous work on rhodamine 6G [16], a molecule of similar size, structure and charge, which is consistent with a chemically intuitive model to be discussed later. The system is assumed to be invariant under rotation about the laboratory Z axis, described the angle ϕ, as a consequence of the in-plane isotropy of a liquid interface.

The polarization of the second harmonic radiation from the air/water interface was measured by the null angle technique to be 19° ± 2°. This would correspond to a molecular axis tilt angle (θ) of 42° ± 1°, assuming a sharp distribution of molecular orientations. The effect of including a contribution from $\alpha^{(2)}_{zxx}$, is to reduce θ, bringing the molecule into a more upright position.

The polarization of the second harmonic fields radiated from the octane/water interface, corrected for effects of refraction and angle of incidence, yields a molecular axis tilt angle of 42° ± 1°, which is close to that found for the air/aqueous interface. We obtain the same orientation for malachite green at the pentadecane/water interface. In addition we find that the SH signal from the alkane/aqueous interface is more than an order of magnitude greater than for the air/aqueous interface at a similar bulk malachite green concentration. This result, which indicates a large increase in the population at the alkane/water interface relative to the air/aqueous interface, points to a favorable interaction of malachite green with the alkane phase, supporting the expectation of an interface geometry in which the hydrophobic phenyl group projects into the alkane phase.

This interfacial geometry is further supported by our SH measurements of the adsorption isotherm at the different interfaces, i.e. the SH signal as a function of malachite green concentration in the bulk aqueous solution [56]. The isotherm is well described by Langmuir adsorption. The Gibbs free energy of adsorption (ΔG) reveals a greater driving force for adsorption to the pentadecane/water interface ($\Delta G = -11.2 \pm 0.6$ kcal/mol) than for adsorption to the air/water interface ($\Delta G = -9.0 \pm 0.5$ kcal/mol). This result is chemically intuitive in view of the significantly greater solubility of benzene in alkanes as opposed to water. Thus one would expect an attractive interaction between the phenyl group of MG and the alkane phase at the interface.

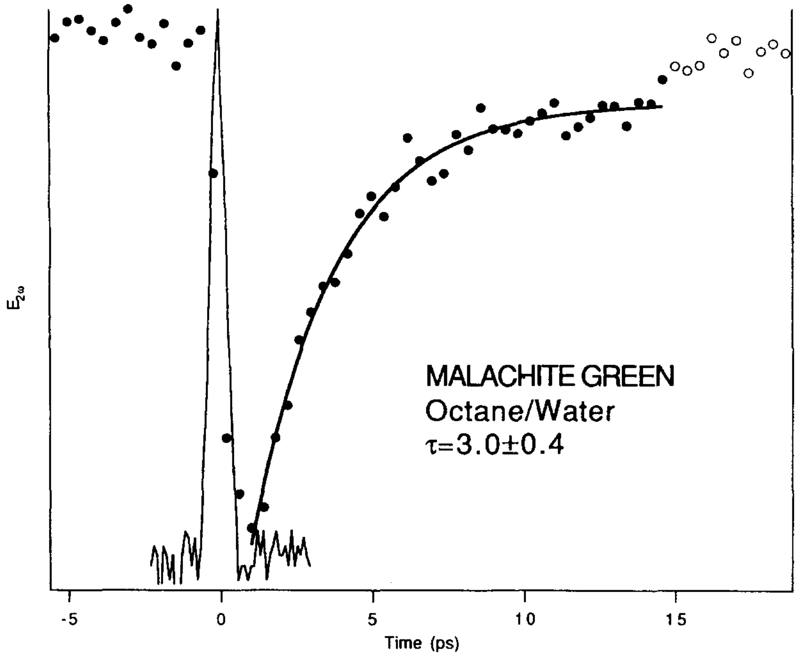

Fig. 3. TRSHG dynamics of malachite green at octane/water interface. The solid line is a single exponential fit to the data. The last ten points ($t > 15$ ps, open circles) are obtained with the pump blocked, thus showing a small offset discussed in the text. The sum frequency signal due to the simultaneous presence of the pump and probe beams is also shown to indicate the instrument response function.

3.2. Frictional resistance and adsorbate geometry at aqueous interfaces

Based on the orientational results and the adsorption energetics we infer that the phenyl group projects into the octane and pentadecane phases with the same orientation while the charged anilino groups project into the water phase. This interface geometry for malachite green is consistent with a model with a geometry based on simple chemical considerations. For this geometry we expect that the twisting of the phenyl group about the central carbon–phenyl bond and the twisting of the anilino groups about their respective central carbon–anilino bonds would be very sensitive to the frictional properties of the phase in which these groups are located, namely the alkane and water phases. Thus the frictional resistance to the twisting of the phenyl group should be much greater at the pentadecane/water interface than the octane/water interface based on the sixfold greater viscosity of pentadecane relative to octane. Contrary to this expectation, we found that the isomerization dynamics differed by only 20% at the two alkane/aqueous interfaces (Figs. 3 and 4). The relaxation times of 3.0 ± 0.4 and 3.6 ± 0.3 ps at the octane/aqueous, and pentadecane/aqueous interfaces, respectively, suggest that the photoisomerization dynamics of malachite green does not depend significantly on the rotation of the phenyl group. This is contrary to the generally accepted model which assumes that the synchronous twisting of all the aromatic moieties determines the rate of isomerization [25,27,57,58]. Our results suggest that it is the nitrogen containing dimethylaniline moieties that determine the isomerization rate. Because these more hydrophilic moieties project into the aqueous phase, we infer that it is the frictional resistance in the aqueous phase that is chiefly responsible for the observed relaxation times. The similar relaxation times (within 20% of each other) for the two alkane/water interfaces suggests that the structure of water at these interfaces is essentially the same. On the other hand the different relaxation times at the air/water and alkane/water interfaces suggest that

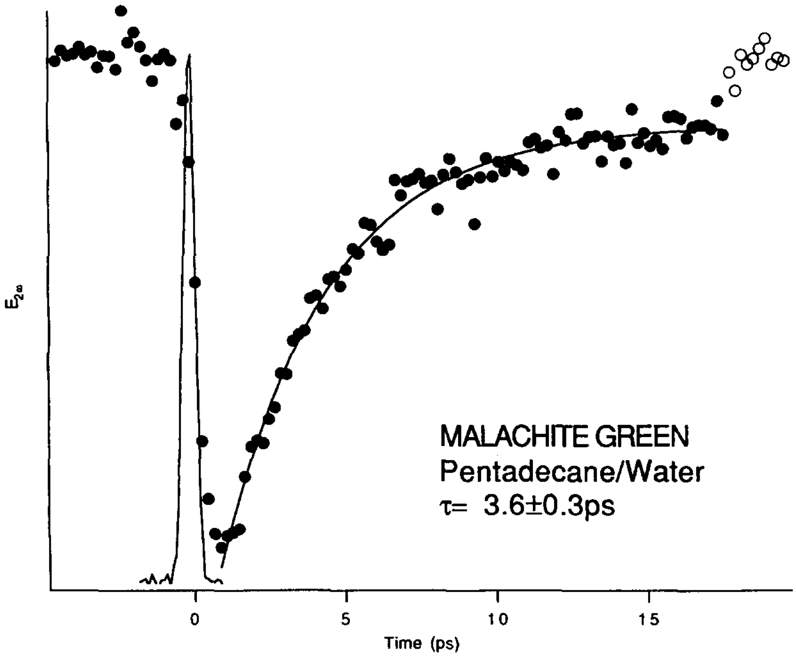

Fig. 4. TRSHG dynamics of malachite green at pentadecane/water interface. The solid line is a single exponential fit to the data. The last ten points ($t > 15$ ps, open circles) are obtained with the pump blocked, thus showing a small offset discussed in the text. The instrument response function is also shown.

there could be differences in the water structure at the various aqueous interfaces, though probably not very large ones. Although the orientation of malachite green is similar at the various interfaces, which indicates that the differences in relaxation times are not due to any dependence of the friction on the interfacial orientation, it is possible that the vertical position of malachite green could differ for air/water and alkane/water interfaces. It would not be unlikely for the phenyl group to project further into the alkane phase, because of van der Waals interactions with the alkane molecules, than into the air phase. Thus the anilino groups would be located in that part of the water phase closer to the alkane interface, which could have a different structure and thus exert a different frictional resistance to the twisting motions. Theoretical studies, based on molecular dynamics simulations, concluded that the structure of water at the air/aqueous and alkane/aqueous interfaces is similar [59,60]. We cannot establish on the basis of these experiments whether the different relaxation times are due to the structure of water being different at the alkane/water and air/water interfaces or the structure of water being the same at these interfaces and the different relaxation times arise from the different positions of malachite green at the air/water and alkane/water interfaces. In any event the results suggest that there is not a major difference in the water structure at the air/aqueous and alkane/aqueous interfaces.

Unlike the air/aqueous and alkane/aqueous interfaces, the phenyl group as well as the dimethylaniline groups must be immersed in the water phase at the silica/aqueous interface. We find that the isomerization dynamics (Fig. 5) is slower (5.5 ± 1.0 ps) than at the air/aqueous and alkane/aqueous interfaces, indicating that there is either a specific interaction of malachite green with charged silanol groups or that the structure of water at the silica interface in the vicinity of malachite green is different from that at the alkane and air interfaces [61]. As noted earlier the silica/aqueous interface experiments were carried out in a pH range of 2.4 to 3.6 to avoid the formation of MG^{2+}, which becomes significant at

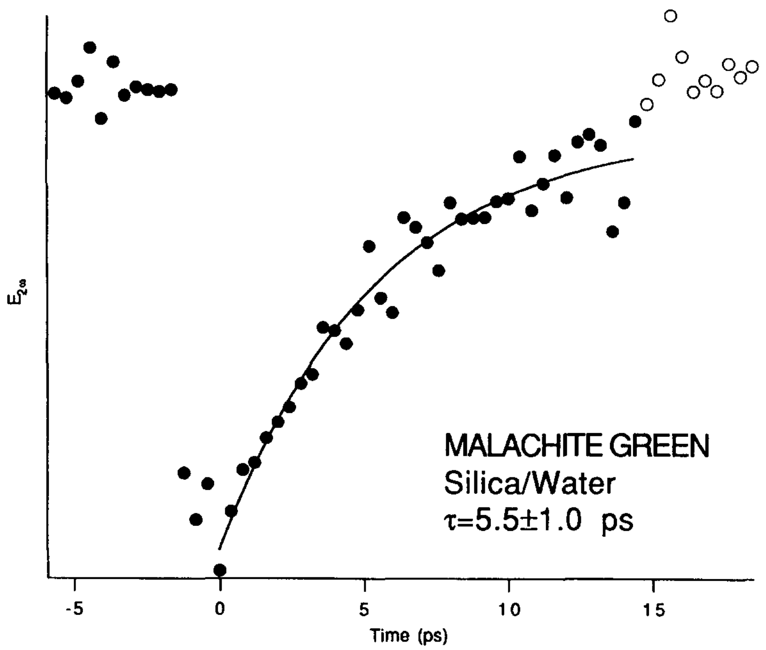

Fig. 5. TRSHG dynamics of malachite green at silica/water interface. The solid line is a single exponential fit to the data. The last ten points ($t > 15$ ps, open circles) are obtained with the pump blocked, thus showing a small offset discussed in the text. Bulk pH = 3.6.

$pH < 2$ and carbinol (MGOH) which becomes the dominant form at $pH > 7$. Although the MG^+ is the dominant from (> 95%) in the pH range of 2.4 to 3.6, the silica surface changes to some extent over this pH range due to the ionization of the –SiOH groups. Based on our work on the pK_a of the –SiOH groups at the silica/aqueous interface we estimate that roughly 1% of the silanols ($\sim 5 \times 10^{12}$ $-SiO^-/cm^2$) are ionized in this pH range. The increase in the SiO^- density at the higher end of the pH range we have studied increases the attractive interaction of the silica with the cation MG^+. This increased attractive interaction results in an increased MG^+ population at the interface, which is reflected in the larger SH signal found at pH 3.6 relative to pH 2.4. Although the SH signal increased by a factor of ten we found that neither the dynamics nor the orientation of MG^+ changed across this pH range (pH = 2.4–3.6). These latter results indicate that the interactions of MG^+ with the interfacial moieties, which includes the interfacial water, the SiO^- and the SiOH groups, is not changing with pH from pH 2.4 to 3.6. It therefore seems plausible that the MG^+ are preferentially adsorbed to the location of the $-SiO^-$ moieties and that increasing the density of $-SiO^-$ groups (by raising the pH) increases the population of adsorbed MG^+ without changing the local environment of the interfacial MG^+. Thus, the orientation of MG^+ and the photoisomerization dynamics remain unchanged even though the MG^+ population increases across this pH range.

Comparing our results with the fluorescence studies of malachite green at the silica/aqueous interface [26], we note that the 350 ps instrument function in the fluorescence studies precluded measurement of the rapidly relaxing populations that we observe. The long lifetimes detected in the fluorescence experiments could correspond to the small residual signal we observe, which on the picosecond timescale appears as a constant offset and thus does not contribute to the dynamics observed in TRSHG experiments.

It is furthermore of interest to note that although the phenyl group and the dimethylaniline groups are immersed in the aqueous phase, the isomerization dynamics at the silica/aqueous interface are different (slower) than in the bulk aqueous phase. This result has a bearing on some experimentally based inferences, that water structure and therefore viscosity are greater at the silica/aqueous interface than in the bulk aqueous solution [20,62–64].

3.3. Comparison of isomerization rates at the air/aqueous interface

It is of some interest that, compared with bulk aqueous lifetimes, the increase in lifetime observed for malachite green at aqueous interfaces is opposite to the observed decrease in lifetime of the activated photoisomerization dynamics of the cyanine dye DODCI at the air/aqueous interface [14]. For malachite green and DODCI we believe that the molecular environment, orientation and solvent structure in the vicinity of the different chromophores of the two molecules dictate the observed interfacial behavior. The expected orientation of DODCI leads to one end of the molecule pointing away from the bulk water phase towards the air, analogous to what is observed for the phenyl group of malachite green. For DODCI the photoisomerization can be achieved by the motion of one end of the cyanine dye about its methylene bonds, through the air side of the air/aqueous interface, which is a region of low solvent coupling. However, for malachite green the motion that effects the isomerization is that of the anilino groups, which are immersed in the aqueous phase, which is a region of strong coupling to the interfacial water molecules. Thus the friction experienced by DODCI and malachite green is different though they are both at air/aqueous interfaces. With respect to the effects of interfacial solvent polarity we would anticipate that the polarity experienced by DODCI would be less at the air aqueous interface than in the bulk aqueous phase because solvation of DODCI surrounded by water molecules should be greater in the bulk solution. Based on bulk studies we expect the barrier for DODCI isomerization would be higher at the less polar interface and therefore the kinetics would be slower. Our experimental results are opposite to this, which suggests that it is the decreased friction and not the barrier that yields the faster rate for DODCI isomerization at the interface. Theoretical studies, based on molecular dynamics simulations, indicate an increase in the isomerization rate in the strong coupling limit, which is attributed to fewer barrier recrossings in the presence of reduced interfacial solvent density [65]. With respect to malachite green, which undergoes a barrierless isomerization, we ascribe the slower kinetics to the increased structure at the aqueous interface, and thus the increased friction experienced by the dimethylaniline groups that project into the aqueous phase.

4. Conclusion

We have investigated the dynamics of a barrierless chemical reaction, the photoisomerization of malachite green, at air/aqueous, alkane/aqueous and silica/aqueous interfaces. The dynamics are found to be slower at all interfaces than in the bulk solution but surprisingly are not sensitive to the viscosity of the alkane phase at the various alkane/aqueous interfaces. The orienting property of the interface enables the relative contributions of the various aromatic groups of malachite green, namely the hydrophobic phenyl group projecting into the alkane phase and the charged hydrophilic dimethylaniline groups projecting into the aqueous phase, to be determined in the isomerization process. Contrary to current models of isomerization of triphenylmethane dyes, we suggest, on the basis of the TRSHG experiments, that rotation about the central carbon–phenyl bond is not significant in the isomerization process. The twisting motions of the dimethylaniline groups are the dominant pathway governing the photoisomerization dynamics. The slower isomerization dynamics at the silica/aqueous interface are consistent with the idea that water is more structured in the neighborhood of the solid (silica)/aqueous interface and thus the friction is greater than in the bulk aqueous phase. Based on these studies of malachite green and DODCI, it is suggested that the friction experienced at an interface must be considered in terms of the orientation of the molecule at the interface, the preferred location of the various parts of the adsorbed molecule, the local solvent structure and most importantly the particular motion involved in the chemical or physical process.

Acknowledgements

The authors wish to thank the Division of Chemical Science of the Department of Energy for their support and the National Science Foundation for their equipment support.

References

[1] Y.R. Shen, Ann. Rev. Phys. Chem. 40 (1989) 327.
[2] G.L. Richmond, J.M. Robinson and V.L. Shannon, Progr. Surface Sci. 28 (1988) 1.
[3] C.D. Bain, P.B. Davies, T.H. Ong, R.N. Ward and M.A. Brown, Langmuir 7 (1991) 1563.
[4] G. Berkovic, Physica A 168 (1990) 140.
[5] T.F. Heinz, in: Nonlinear surface electromagnetic phenomena, eds. H.-E. Ponath and G.I. Stegeman (Elsevier, Amsterdam, 1991).
[6] K.B. Eisenthal, Ann. Rev. Phys. Chem. 43 (1992) 627.
[7] K.B. Eisenthal, Accounts Chem. Res. 26 (1993) 636.
[8] R.M. Corn and D.A. Higgins, Chem. Rev. 94 (1994) 107.
[9] J.M. Hicks, K. Kemnitz, K.B. Eisenthal and T.F. Heinz, J. Phys. Chem. 90 (1986) 560.
[10] T. Rasing, Y.R. Shen, M.W. Kim, J.P. Valint and J. Bock, Phys. Rev. A 31 (1985) 537.
[11] A. Castro, K. Bhattacharyya and K.B. Eisenthal, J. Chem. Phys. 95 (1991) 1310.
[12] X. Zhao, S. Subrahmanyan and K.B. Eisenthal, Chem. Phys. Letters 171 (1990) 558.
[13] D. Zhang, J.H. Gutow, K.B. Eisenthal and T.F. Heinz, J. Chem. Phys. 98 (1993) 5099.
[14] E.V. Sitzmann and K.B. Eisenthal, J. Phys. Chem. 92 (1988) 4579.
[15] E.V. Sitzmann and K.B. Eisenthal, J. Chem. Phys. 90 (1989) 2831.
[16] A. Castro, E.V. Sitzmann, D. Zhang and K.B. Eisenthal, J. Phys. Chem. 95 (1991) 6752.
[17] D. Mobius, R.C. Ahuja, G. Caminati, L. Chi, W. Cordroch, Z. Li and M. Matsumoto, in: Proc. Dyn. Mech. Photoinduced Electron Transfer Relat. Phenom., Yamada, Japan, 1991, eds. N. Mataga, T. Okada and H. Masuhara (North-Holland, Amsterdam, 1992) p. 377.
[18] P.A. Anfinrud, D.E. Hart, J.F. Hedstrom and W.S. Struve, J. Phys. Chem. 90 (1986) 5887.
[19] S.R. Meech and K. Yoshihara, Chem. Phys. Letters 174 (1990) 423.
[20] M. Yanagimachi, N. Tamai and H. Masuhara, Chem. Phys. Letters 201 (1993) 115.
[21] S.R. Meech and K. Yoshihara, J. Phys. Chem. 94 (1990) 4913.
[22] P. Guyot-Sionnest, Phys. Rev. Letters 64 (1991) 2156.
[23] M. Morin, N.J. Levinos and A.L. Harris, J. Chem. Phys. 96 (1992) 3950.
[24] V. Sundstrom and U. Aberg, J. Mol. Liquid 57 (1993) 149.
[25] D.F. Duxbury, Chem. Rev. 93 (1993) 381.
[26] M.A. Bell, B. Crystall, G. Rumbles, G. Porter and D.R. Klug, Chem. Phys. Letters 221 (1994) 15.
[27] K. Kemnitz and K. Yoshihara, Chem. Letters (1990) 1789.
[28] K. Kemnitz and K. Yoshihara, J. Phys. Chem. 94 (1990) 8805.

[29] M.J.E. Morganthaler and S.R. Meech, Chem. Phys. Letters 202 (1993) 57.

[30] M.J.E. Morganthaler and S.R. Meech, in: Ultrafast phenomena VIII, eds. J.L. Martin, A. Migus, G.A. Mourou and A.H. Zewail (Springer, Berlin, 1993) p. 606.

[31] D.A. Cremers and M.W. Windsor, Chem. Phys. Letters 71 (1980) 27.

[32] M.M. Martin, E. Breheret, F. Nesa and Y.H. Meyer, Chem. Phys. 130 (1989) 279.

[33] C.J. Mastrangelo and H.W. Offen, Chem. Phys. Letters 46 (1977) 588.

[34] L.A. Brey, G.B. Schuster and H.G. Drickamer, J. Chem. Phys. 67 (1977) 2648.

[35] D. Ben-Amotz, R. Jeanloz and C.B. Harris, J. Chem. Phys. 86 (1987) 6119.

[36] M. Vogel and W. Rettig, Ber. Bunsenges. Phys. Chem. 89 (1985) 962.

[37] W. Rettig, Appl. Phys. B 45 (1988) 145.

[38] G. Oster and Y. Nishijima, J. Am. Chem. Soc. 78 (1956) 1581.

[39] T. Förster and G. Hoffmann, Z. Physik. Chem. 75 (1971) 63.

[40] B. Bagchi, G.R. Fleming and D.W. Oxtoby, J. Chem. Phys. 78 (1983) 7375.

[41] D. Ben-Amotz and C.B. Harris, J. Chem. Phys. 86 (1987) 5433.

[42] R.A. Engh, J.W. Petrich and G.R. Fleming, J. Phys. Chem. 89 (1985) 618.

[43] J.J. Song, J.H. Lee and M.D. Levenson, Phys. Rev. A 17 (1978) 1439.

[44] R. Trebino and A.E. Siegman, J. Chem. Phys. 79 (1983) 3621.

[45] A.E. Siegman, in: Applications of picosecond spectroscopy to chemistry, ed. K.B. Eisenthal (Reidel, Dordrecht, 1984).

[46] H. Lu, F.H. Long and K.B. Eisenthal, J. Opt. Soc. Am. B 7 (1990) 1511.

[47] S.W. Ong, X.L. Zhao and K.B. Eisenthal, Chem. Phys. Letters 191 (1992) 327.

[48] A.W. Adamson, Physical chemistry of surfaces, 4th Ed. (Wiley, New York, 1982).

[49] S. Saikan and J. Sei, J. Chem. Phys. 79 (1983) 4154.

[50] A. Migus, A. Antonetti, J. Etchepare, D. Hulin and A. Orszag, J. Opt. Soc. Am. B 2 (1985) 584.

[51] A. Mokhtari, L. Fini and J. Chesnoy, J. Chem. Phys. 87 (1987) 3429.

[52] T.F. Heinz, H.W.K. Tom and Y.R. Shen, Phys. Rev. A 28 (1983) 1883.

[53] D.A. Higgins, M.B. Abrams, S.K. Byerly and R.M. Corn, Langmuir 8 (1992) 1994.

[54] D.C. Nguyen, R.E. Muenchausen, R.A. Keller and N.S. Nogar, Opt. Commun. 60 (1986) 111.

[55] H. Goldstein, Classical mechanics (Addison-Wesley, Reading, 1980).

[56] A. Castro, E.V. Sitzmann, D. Zhang and K.B. Eisenthal, Chem. Phys. Letters 163 (1989) 412.

[57] D. Magde and M.W. Windsor, Chem. Phys. Letters 24 (1974) 144.

[58] D. Magde and M.W. Windsor, Chem. Phys. Letters 71 (1980) 27.

[59] A. Pohorille and M.A. Wilson, J. Mol. Struct. 284 (1993) 271.

[60] A. Pohorille and M.A. Wilson, in: Reaction dynamics in clusters and condensed phases, eds. J. Jortner et al. (Kluwer, Dordrecht, 1994) p. 207.

[61] E. Borguet, X. Shi and K.B. Eisenthal, in: Ultrafast phenomena IX, eds. P.F. Barbara, W.H. Knox, G. Mourou and A.H. Zewail (Springer, Berlin, 1994) p. 304.

[62] Q. Du, E. Freysz and Y.R. Shen, Phys. Rev. Letters 72 (1994) 238.

[63] T.G. Fillingim, S.-B. Zhu, S. Yao, J. Lee and G.W. Robinson, Chem. Phys. Letters 161 (1989) 444.

[64] M.F. Toney, J.N. Howard, J. Richer, G.L. Borges, J.G. Gordon, O.R. Melroy, D.G. Wiesler, D. Yee and L.B. Sorensen, Nature 368 (1994) 444.

[65] I. Benjamin and A. Pohorille, J. Chem. Phys. 98 (1993) 236.